Detailed Characterization of Inspection Tools: Capabilities and Limitations of the KLA 576

J. Heumann[a], R. Moses[a], C. Holfeld[a], N. Schmidt[b], C. Aquino[b]
[a] Advanced Mask Technology Center, Rähnitzer Allee 9, 01109 Dresden, Germany
[b] KLA-Tencor Corporation, 160 Rio Robles, San Jose, CA 95134-1809, USA

ABSTRACT

In mask fabrication pattern-inspection is a key step. It ensures mask quality is being met according to the customer defect criteria. Tool selection is based on a comparison between customer requirements and tool capabilities. Inspection tools are typically specified by a minimum feature size at which a certain minimum defect size can be achieved. Mask shops on the contrary manufacture masks for a wide range of feature and defect sizes. As a consequence detailed tool characterizations are needed, which go beyond the typical tool specifications. In this paper characterization results for three KLA 576 inspection systems are presented. Defect sensitivity was studied for the pixels named P125 and P90 in combination with the so-called die-to-die (D2D) and die-to-database (D2Db) algorithms using standardized programmed defect masks. The good correlation of the qualification data made modeling of the tool behavior possible. The modeling parameters were used to compare tool-to-tool and plate-to-plate variations as well as specified and actual tool performance. For a variety of mask types, such as Chrome-on-Glass (COG) masks, embedded phase shift masks at a lithography wavelength of 193 nm (EPSM-193), and extreme ultra-violet (EUV) masks, the optical contrast was studied over a wide range of feature sizes. From the resultant data material dependence and image contrast below the minimum feature size was evaluated.

Keywords: mask inspection, mask defect, defect sensitivity, feature size

INTRODUCTION

An inspection tool's performance is typically characterized by two numbers. These are the minimum feature size and the minimum defect size. The minimum feature size represents the smallest feature size, which can still be well resolved by the tool's imaging optics. In turn the minimum defect size represents the defect size, which, if located in features above the minimum feature size, can still be found reliably by the inspection tool.

The minimum feature and defect size are dependent on tool's imaging optics and the defect detection algorithm. The optics determines how well a feature/defect can be resolved. The defect detection algorithm typically subtracts a reference from a test image. Without any defects the so-called difference image shows a constant intensity. A defect becomes visible through a deviation of image intensity. To control the defect sensitivity user-configurable thresholds are applied, which define the maximum allowable intensity deviation. The so-called detectors define the exact method, by which the thresholds are applied to the difference image. The minimum detectable defect size is determined by the noise floor of the difference image, which in turn is influenced by the image resolution. As a consequence the minimum feature size is only determined by the imaging optics, whereas the minimum defect size is determined both by the imaging optics as well as the detection algorithm.

A mask shop manufactures masks over a wide range of feature sizes and defect sizes. In order to optimize yield the inspection tool is tuned to the customer specifications. In practice this means choosing the proper image resolution (pixel), algorithm, as well as detector settings. As the tool vendor typically does not characterize the performance below specification, a mask shop needs to perform a detailed characterization of the inspection system. For this purpose a standardized programmed defect mask is chosen. Because of the large parameter space (pixel, algorithm, and detector settings) appropriate tool settings are traditionally found upon customer request. In order to find the optimum settings the tool is characterized in a certain range. With increasing number of feature sizes and defect sizes the tool characterizations become time consuming.

The development of new mask technologies often requires inspection of feature sizes below the specified minimum feature size. Studying the defect sensitivity at different feature sizes requires the characterization of numerous defects . An alternative approach can be taken by studying the image contrast at different feature sizes.

This paper shows results of a detailed tool characterization for three different KLA 576 inspection systems. Each tool was characterized for the pixels P90 and P125 in combination with the algorithms D2D and D2Db. The resultant data

was analyzed for correlations and eventually modeled. The modeling parameters were used to determine the range of useable defect sizes, tool stability with time, tool-to-tool variations, as well to compare calculated and specified minimum defect size. In order to gain an understanding of the minimum defect size below the minimum feature size, the image contrast for P90 was studied over a wide range of feature size for COG, EPSM-193 and EUV masks.

EXPERIMENTAL

I. Defect sensitivity

The three KLA 576s were characterized using KLA standard programmed defect masks called SPICA (see Tab. 1).

Tool name	Tool type
INS101	KLA 576
INS106	KLA 576
INS107	KLA 576

Tab. 1: List of tools characterized in this study.

For each tool the following combination of pixels and algorithms were characterized:

Pixel	Algorithm	SPICA mask type
P90	D2D	COG
P90	D2D	EPSM-193
P90	D2Db	COG
P125	D2D	COG
P125	D2D	EPSM-193
P125	D2Db	COG

Tab. 2: Combination of pixels and algorithms characterized for each tool.

No data is shown for P90 and P125 in combination with the D2Db algorithm for EPSM-193 masks, as these masks are typically run in a so-called tritone mode, which is currently not specified by KLA.
The D2D and D2Db algorithms have two main software detectors called HiRes1 and HiRes2. HiRes1 is the main pattern detector, whereas HiRes2 is specifically tuned to find single pixel variations. Both detectors act independent of each other, which allows studying one detector, while the other one is turned off. In order to limit the amount of testing, HiRes1 and HiRes2 were studied for the following settings.

Detector	Detector settings used														
HiRes1	100	90	80	70	60	50	40	30	20	10	0	0	0	0	0
HiRes2	0	0	0	0	0	0	0	0	0	0	100	80	60	40	20

Tab. 3: Detector settings studied for each combination of pixel and algorithm.

The inspection tools were delivered with different versions of SPICA. In the course of this study the following five different SPICA plates were used.

SPICA name	Mask type
SPICA400-COG v3	COG
SPICA400-193 v3	EPSM-193
SPICA400-COG v4	COG
SPICA400-193 v4	EPSM-193
SPICA200 v6	COG & EPSM-193

Tab. 4: List of SPICA masks used for tool characterization.

Each SPICA mask contains the following 15 types of defects:

Defect type	Defect category
Extension on horizontal line	On-edge defect
Intrusion on horizontal line	On-edge defect
Extension on diagonal line	On-edge defect
Intrusion on diagonal line	On-edge defect
Extension on corner	On-edge defect
Intrusion on corner	On-edge defect

Defect type	Defect category
Pin dot	Isolated defect
Pinhole	Isolated defect
Over size	CD variation
Under size	CD variation
Elongation of line-end	Line-end
Truncation of line-end	Line-end
Partial misplacement of feature	Misplacement
Full misplacement of feature	Misplacement

Tab. 5: List of programmed defect types on SPICA and their corresponding defect category used in this study.

In order to limit the amount of data presented in this paper the defects were grouped into defect categories (see Tab. 5). For each defect type a SPICA200 and SPICA400 contains 30 and 20 different defect sizes, respectively. Each SPICA mask is characterized by taking SEM images for selected "isolated" and "on-edge" defects, which are sized via the so-called "minimum inscribed circle diameter" (MICD) method. In this study all "isolated" and "on-edge" defects, which have not been SEM-sized are ignored, as mask processing causes the actual defect size to differ largely from the design size. For all other defect categories the design sizes are used, as these typically match with the actual defect size.
For each individual tool setting (pixel, algorithm, and detector setting) ten inspections were performed. These inspections were analyzed for determining the capture rate of each programmed defect.

II. Image contrast

The image contrast was studied for COG, EPSM-193, and EUV masks. The patterns were limited to so-called lines&spaces, which had exhibited the high defect printability in previous studies. Images were taken for half-pitches ranging from 100 nm to 800 nm at certain increments. The sizes of the lines and spaces were kept constant at a an aspect ratio of 1:1. The image contrast was studied for the three pixels P90, P125, and P90R. Light calibration was performed using the following black and white values:

	Light calibration gray scale values		
Light level	COG	EPSM-193	EUV
Black	5	40	25
White	248	240	250

Tab. 6: List of image gray scale values for the black and white light levels used for light calibration of COG, EPSM-193, and EUV masks.

The gray scale values for COG and EPSM-193 correspond to the KLA recommended values. The gray scale values for EUV masks were chosen such that for all collected images no clipping of the intensity was observed (intensity values below 0 or above 256). After light calibration optical images were recorded for each pattern (see Fig. 1 left image).

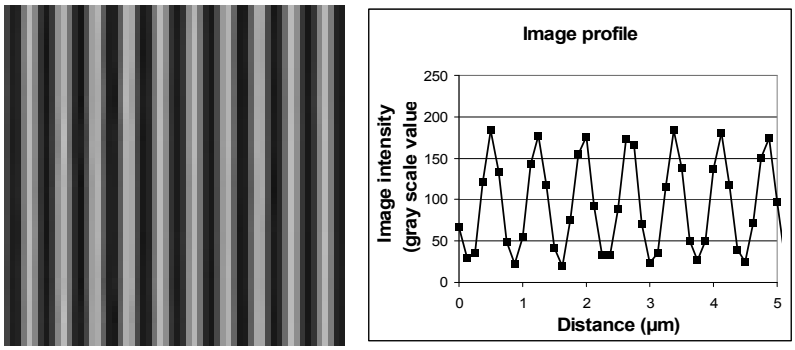

Fig. 1: Left image: Image recorded with P125 for a COG mask with half-pitch of 360nm.
Right image: Intensity profile of the left image drawn perpendicular to the lines.

The resultant images were evaluated plotting profiles perpendicular to the lines (see Fig. 1 right image). From the profiles the intensity maximum (I_{max}) and intensity minimum (I_{min}) were determined. In optics, it is common practice to calculate the image contrast (C) using the following formula:

$$C = \frac{I_{\max} - I_{\min}}{I_{\max} + I_{\min}}$$

However a test and reference image is subtracted, when using the D2D or D2Db algorithm, and defect detection is based on intensity deviations between corresponding pixels of the two images. The defect sensitivity is controlled by a threshold, which defines the maximum allowable intensity deviation not to be considered as defect. The defect detection is therefore not governed by the image contrast of the raw image but the difference image. Defect detection thus is influenced by the intensity difference (I_{diff}), rather than the image contrast (C). The I_{diff} values were normalized relative to the maximum-recorded intensity difference (I^{max}_{diff}).

$$I_{diff} = I_{\max} - I_{\min}$$

$$I^{*}_{diff} = \frac{I_{diff}}{I^{\max}_{diff}}$$

The resultant I^{*}_{diff} value were plotted over the corresponding half-pitch.

RESULTS & DISCUSSION

I. Defect sensitivity

For each tool setting the smallest defect size detected with a capture rate of 100% was identified for every individual defect type. The resultant data was plotted versus the corresponding detector setting (see Fig. 2 left image).

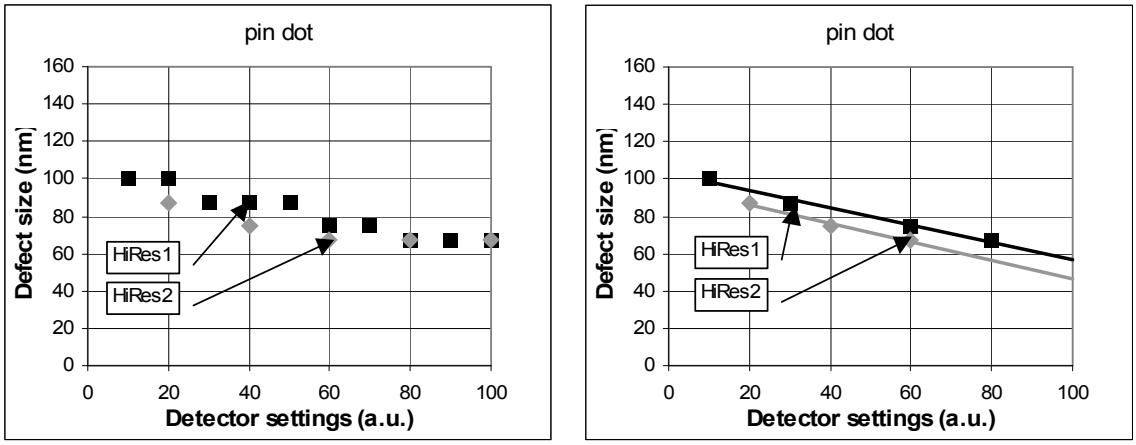

Fig. 2: Smallest pin dot of a SPICA400-COG v4 found with 100 % capture rate
plotted versus the corresponding HiRes1 and HiRes2 detector settings for P90 D2Db.
Left image: Plot including all measurement points.
Right image: Plot for selected measurement points and corresponding "least-square-fitted" line.

Due to the incremental change in programmed defect sizes, the smallest detected defect size was often identical for two or more detector settings (see Fig. 2 left image). For identical defect sizes the measurement point with the smallest detector setting represents the actual defect sensitivity most accurately. As a consequence all other measurement points were eliminated (see Fig. 2 right image). The resultant data exhibited a linear correlation between defect size and detector settings. For the "least-square-fitted" data the residual values (R^2) were typically above 0.95. In conclusion the detector behavior (HiRes1 or HiRes2) could be modeled using a linear function (defect size = a * detector setting + b). The corresponding slope (a) and y-intercepts (b) were determined for each detector. To calculate the actual defect size the minimum value of each detector (HiRes1 and HiRes2) was used, as both detectors behave independently.

$$Defect\_size = Min\begin{pmatrix} a_1 * Hi\,\mathrm{Re}s1 + b_1 \\ a_2 * Hi\,\mathrm{Re}s2 + b_2 \end{pmatrix}$$

For each combination of tool, pixel, and algorithm characterized in this study (see Tab. 1 and Tab. 2) the "linear-fit" parameters were recorded for each type of programmed defects (see Tab. 7).

	HiRes1			HiRes2		
Defect Type	A	B	R^2	A	B	R^2
Pin dot	-0.46	103	0.987	-0.5	96.3	0.987
Pinhole	-1.14	295	0.956	-0.81	256	0.989
Extension on horizontal line	-0.946	148	0.99	-0.975	155	0.921
Intrusion on horizontal line	-1.08	166	0.953	-0.856	152	0.904
Extension on diagonal line	-0.898	138	0.968	NA	NA	NA
Intrusion on diagonal line	-1	159	0.968	NA	NA	NA
Extension on corner	-1.15	178	0.995	NA	NA	NA
Intrusion on corner	-1.05	154	0.975	NA	NA	NA
Over size	-1.5	195	1	NA	NA	NA
Under size	-1.5	195	1	NA	NA	NA
Elongation of line-end	-0.823	108	0.988	NA	NA	NA
Truncation of line-end	-0.813	104	0.976	NA	NA	NA
Partial misplacement of feature	-0.823	103	0.988	NA	NA	NA
Full misplacement of feature	-0.813	104	0.976	NA	NA	NA

Tab. 7: “Linear fit” parameters for each defect type on a SPICA400-COG v4 for INS107 using P90 D2Db.

The HiRes2 detector was found to only have a measurable influence on pin dots, pinholes, as well as extensions and intrusions on horizontal lines. The low performance on extension and intrusion on diagonal lines as well as line-end defects is currently under investigation. For CD variations and misplacement-defects the low defect sensitivity is explained by the detector intent, as HiRes2 is designed to only find single-pixel intensity deviations.
The usable range of defect sizes is determined by the difference between the maximum and minimum calculated defect size (see Tab. 8).

Pixel	**Algorithm**	**Av. range of defect size (nm)**
P90	D2D	67
P90	D2Db	106
P125	D2D	86
P125	D2Db	157

Tab. 8: Average useable range of defect sizes
for different pixels and algorithms for COG masks.

For COG masks the range of useable defect sizes depends on pixel and algorithm. The largest range of 157 nm is achieved for P125 D2Db. On average P125 exhibits a 35 nm higher defect range than P90. In practice the pixel selection is mostly driven by mask feature size. Thus the increase in range will have no influence on pixel selection. D2Db on average exhibits a 55 nm higher range of defect sizes than D2D. In practice this means that above a certain defect size only D2Db can be used.
The quality of the “linear fitted” data allows studying parameters such as tool stability and the tool-to-tool variation. For the tool characterizations different SPICA plates were used at different stages of this study (see Tab. 9)

Tool name	Time of tool characterization	SPICA used for tool characterization	Tool stability	Tool-to-tool variation
INS101	after final acceptance	SPICA400-COG v3		x
		SPICA400-193 v3		x
INS106	after final acceptance	SPICA400-COG v3		x
		SPICA400-193 v3		x
INS107	at factory acceptance	SPICA400-193 v4	x	
		SPICA400-COG v4	x	
INS107	after final acceptance	SPICA400-193 v4	x	
		SPICA400-COG v4	x	
INS107	after upgrade	SPICA200-COG v6		

Tab. 9: List of tools, time of tool characterization, and the SPICA mask, which has been used for the characterization. The crosses mark the characterization data, which has been used to study tool stability and tool-to-tool variation.

Due to the variety of tools and SPICA plates used, there exists only a limited set of characterizations, which could be compared directly. To study the tool stability the results of the INS107 tool characterization before and after final acceptance were used. To study the tool-to-tool variation the results of the INS101 and INS106 after final acceptance were used. Comparing the individual fit parameters would have been the beyond the scope of this paper. To limit the presented data only the calculated minimum defect sizes are compared.

I.I. Tool stability

INS107 was characterized using a SPICA400-COG v4 and SPICA400-193 v4 before and after installation. The fit parameters were used to calculate the minimum defect size at factory and final acceptance. For each defect category the average value over each defect type was computed. With only two data points per defect category there exists only limited statistics. Rather than calculating the standard deviation, the difference was computed to determine the tool variation at both stages (see Tab. 10). This method has the advantage that a systematic deviation is more readily noticeable by the sign.

		P125		
		D2D		D2Db
		EPSM-193	COG	COG
Difference between factory & final acceptance	CD var	2.10	0.00	-4.50
	Isolated	-2.70	-1.75	-4.43
	Line end	0.00	0.05	7.50
	Misplace	0.00	3.00	1.00
	On-edge	-0.68	3.83	0.50

Tab. 10: Difference between minimum calculated defect size before and after tool installation for different defect categories (rows) and certain combinations of P125 algorithms and mask types (columns).

The maximum absolute difference is observed for COG line-end defects for P125 D2Db (7.5 nm). Best average performance is observed for P125 D2D on EPSM-193 (lowest column average) as well as misplacement defects (lowest row average). In general no pattern signature was noticeable. The average absolute difference was calculated to be 2.1 nm.

I.II. Tool-to-tool variation

INS101 and INS106 both were characterized using a SPICA400-COG v3 and SPICA400-193 v3 at final acceptance. Again the fit parameters were used to calculate the minimum defect sizes. The difference was computed to determine the tool-to-tool variation.

		P125		
		D2D		D2Db
		EPSM-193	COG	COG
Difference between INS106 & INS101	CD var	4.15	4.00	3.00
	Pinholes	NA	-16.30	1.00
	Line end	0.70	0.80	0.50
	Misplace	1.15	-3.70	3.00
	On-edge	2.77	-0.80	2.50

Tab. 11: Difference between minimum calculated defect size for INS101 and INS106 at final acceptance for different defect categories (rows) and certain combinations of P125 algorithms and mask types (columns).

No fit parameters could be determined for pin dots as well as EPSM-193 pinholes for P125 D2D, due to a lack of small-programmed defects on the SPICA mask used. The maximum absolute difference is observed for EPSM-193 pinholes (16.3 nm). Best average performance is observed for D2D on EPSM-193 (lowest column average with isolated defects excluded) and line end defects (lowest column average). Again in general no pattern signature was noticeable. The overall absolute average difference was calculated to be 2.8 nm. Assuming that the tool stability falls within the tool-to-tool variation it can be estimated that the tool-to-tool variation is approx. 3 nm.

I.III. Plate-to-plate variation

In order to study the plate-to-plate variation the difference of the average calculated minimum defect size for SPICA400 v3 (INS101 & INS106 characterization at final acceptance) and for SPICA400 v4 (INS107 before and after installation) were calculated.

		P125		
		D2D		D2Db
		EPSM-193	COG	COG
Difference between SPICA400 v3 & SPICA400 v4	CD var	-11.48	-7.00	-2.75
	Pinholes	NA	-22.70	-22.00
	Line end	4.10	3.48	-0.50
	Misplace	-0.63	-0.35	-3.00
	On-edge	-14.99	-1.15	-2.50

Tab. 12: Difference between SPICA400 v3 and SPICA400 v4 calculated from the average minimum defect size for the two characterizations performed with each plate.

Again due to lack of small-programmed defects for SPICA400 v3, no fit parameters could be determined for pin dots as well as EPSM-193 pinholes for P125 D2D. A noticeable difference of -22 nm is observed for COG pinholes. The origin of this difference is currently under investigation. It might be attributed to the shaping of the programmed defects. Apart from pinholes the largest difference is observed for EPSM-193 defects, for which especially CD variation and on-edge defects exhibit a difference of above 10 nm. Again this difference is currently under investigation and might be attributed to the shaping of the programmed defects. With the exclusion of pinholes the calculated minimum defect sizes for SPICA400 v3 is on average 4.3 nm smaller than for SPICA400 v4. This difference is approx. 50 % larger than the previously studied tool-to-tool variation. This means that the plate-to-plate variation is the limiting factor in specifying the actual tool capability.

I.IV. Tool capability margins

In principal the minimum calculated defect size varies with defect type. The KLA specification takes this into consideration by specifying the minimum defect size by defect type. The accuracy of the fit parameters allows comparing the calculated minimum defect size with the specified minimum defect size for each defect type.
The quality of SPICA masks has improved with each new released version. The latest type offers 30 defect sizes for every different defect type. The defect spacing has decreased such that the number of usable measurement points (see

Fig. 2) has increased from approx. 4 to approx. 8 for HiRes1. As a consequence the fit parameters have higher reliability. A comparison of calculated and specified minimum defect size was therefore done for the SPICA200 v6.

		P125			P90		
		D2D		D2Db	D2D		D2Db
		EPSM-193	COG	COG	EPSM-193	COG	COG
Difference between specified & calculated min. defect size	On-edge	15.75	17.53	11.17	16.37	17.30	12.83
	Isolated	24.50	27.50	30.00	NA	33.95	45.70
	CD var	11.50	3.00	5.50	11.25	8.50	3.00
	Misplace	16.30	24.00	23.50	13.60	23.75	22.60
	Line end	19.40	19.00	16.50	17.15	18.35	16.00

Tab. 13: Difference between calculated and specified minimum defect size (sensitivity margin) for INS107 using SPICA200 v6

The largest difference between specified and calculated minimum defect size is observed for isolated defects (average of 32 nm). On average the specified minimum defect size is 15 nm larger than the calculated minimum defect size. In practice this means that the KLA 576 inspection tools perform noticeably better than specified. Taking the tool-to-tool and plate-to-plate variation into consideration (approx. 7.5 nm sum total) the actual performance is approx. 7.5 nm better than specified.

II. Image contrast

The graph below shows the normalized intensity difference (I^*_{diff}) for P90 and P125 for COG and EPSM-193 as well as P90R for EUV masks.

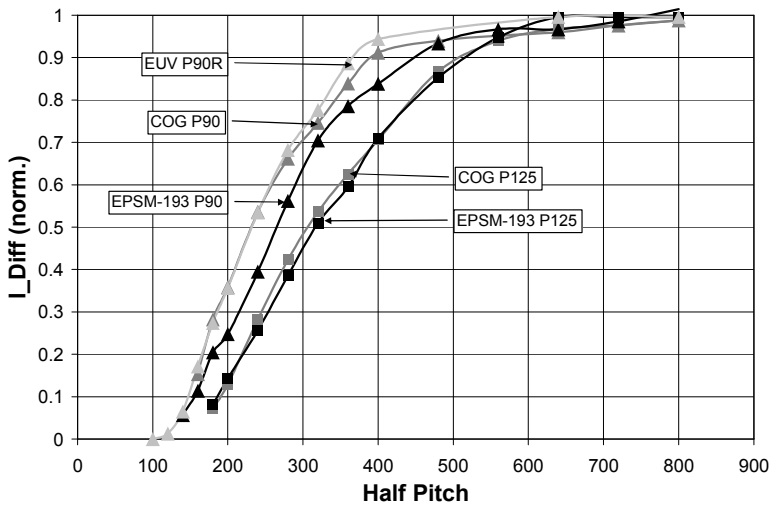

Fig. 3: Intensity difference (I^*_{min}) plotted over half-pitch for lines&spaces for certain pixel (P90, P90R, and P125) and mask material (COG, EPSM-193, and EUV) combinations.

The resultant curves of P125 for COG and EPSM-193 masks as well as of P90R for EUV and of P90 for COG and EPSM-193 overlap within the margin of measurement error. From the overlapping of the curves it was concluded that intensity difference is independent of the mask material. Detection of pattern defects is therefore only influenced by the pixel, the gray scale values used during light calibration, and the actual feature size on the mask.
For P90 and P125 the specified min. half pitch is 350 nm and 250 nm. For both pixels the corresponding I^*_{diff} values are at approx. 0.55. Below these numbers the intensity difference decreases linearly. A direct correlation to the min. defect size below the min. feature size with the available data could not be established, but is currently under investigation.

SUMMARY

In the course of this study over 3000 inspections were performed and analyzed. The tool characterizations showed that detector settings have a linear dependence on defect size. The “least-square-fitted” data exhibited on average a residual (R^2 value) of above 0.95. The high accuracy of the fit parameters allows calculating the tool settings over a wide range of defect sizes. The actual applicable range depends on the pixel and algorithms used. For D2Db the range of defect sizes is on average 55 nm larger than for D2D. This means that above a certain defect size only D2Db can be used to match the customer requirements.

The accurate modeling of the tool settings was used to investigate tool stability with time, tool-to-tool variations, and plate-to-plate variations. It was found that before and after tool installation the calculated change in defect sensitivity on average is below 2.1 nm. A tool-to-tool comparison exhibited on average a calculated difference of 2.8 nm. For different versions of SPICA masks on average a variation of 4.3 nm is observed. This concludes that tool stability and tool-to-tool variation is lower than the plate-to-plate variation.

The fitted tool parameters were also used to compare the calculated minimum defect size with the specified minimum defect size. Taking the tool-to-tool variation and plate-to-plate variations into consideration, it was found that the tools on average perform approx. 7.5 nm better than specified.

For features sizes below the specified minimum feature size the intensity difference decreases linearly. The mask material was found to have no influence on the image contrast. A correlation of image contrast and minimum defect size will be the goal of future investigations.